Biochem. J. (1992) 288, 553–564 (Printed in Great Britain)

Expression of a cardiac Ca^{2+}-release channel isoform in mammalian brain

F. Anthony LAI,*†‡ Myrna DENT,* Colin WICKENDEN,* Le XU, † Gouri KUMARI,† Manoj MISRA,§ Hee Bong LEE,† Madhabananda SAR|| and Gerhard MEISSNER†

*MRC National Institute for Medical Research, The Ridgeway, Mill Hill, London NW7 1AA, U.K.,
†Department of Biochemistry and Biophysics, and ||Department of Cell Biology and Anatomy,
University of North Carolina School of Medicine, Chapel Hill, NC 27599, U.S.A., and §Department of Cell Biology,
Duke University Medical Center, Durham, NC 27710, U.S.A.

Mammalian brain possesses ryanodine-sensitive Ca^{2+} channels, which in muscle cells mediate rapid Ca^{2+} release from intracellular stores during excitation–contraction coupling. Analysis of bovine brain ryanodine receptor (RyR) channels suggests specific expression of the cardiac-muscle RyR isoform in mammalian brain. Localization using cardiac-muscle RyR-specific antibodies and antisense RNA revealed that brain RyRs were present in dendrites, cell bodies and terminals of rat forebrain, and highly enriched in the hippocampus. Activity of skeletal-muscle RyR channels is coupled to sarcolemmal voltage sensors, in contrast with cardiac-muscle RyR channels, which are known to be Ca^{2+}-induced Ca^{2+}-release channels. Thus Ca^{2+}-induced Ca^{2+} release from intracellular stores mediated by brain RyR channels may be a major Ca^{2+}-signalling pathway in specific regions of mammalian brain, and hence may play a fundamental role in neuronal Ca^{2+} homoeostasis.

INTRODUCTION

Transient elevations of cytoplasmic free Ca^{2+} induced by release from non-mitochondrial intracellular stores, can be (i) triggered by a change in surface membrane potential, or (ii) mediated by a series of voltage-independent steps via the formation of a chemical second messenger, inositol 1,4,5-trisphosphate (IP_3). The voltage-dependent mechanism of intracellular Ca^{2+} release has been extensively studied in striated muscle, and is commonly referred to as excitation–contraction (E–C) coupling (Catterall, 1991). In E–C coupling, an action potential is propagated along the muscle surface membrane and its infoldings, the transverse tubular (T-) system. On reaching the T-system, the depolarizing signal is communicated to the sarcoplasmic reticulum (SR) and triggers therefrom a large and rapid release of Ca^{2+} ions via a Ca^{2+}-release channel (Lai & Meissner, 1989). Ca^{2+} release from cardiac SR is triggered by extracellular Ca^{2+} ions which enter the muscle cell through voltage-dependent Ca^{2+} channels (Cannell *et al.*, 1987; Näbauer *et al.*, 1989). Skeletal-muscle SR Ca^{2+} release, however, does not require extracellular Ca^{2+}, but rather is believed to be coupled via a direct physical interaction with a voltage-sensing molecule in the T-system (Rios & Pizarro, 1988).

Identification of the plant alkaloid ryanodine as a release-channel-specific probe, has enabled the biochemical isolation (Campbell *et al.*, 1987; Inui *et al.*, 1987*a*,*b*; Lai *et al.*, 1988*a*,*b*), functional reconstitution (Lai *et al.*, 1988*b*; Smith *et al.*, 1988; Anderson *et al.*, 1989) and subsequent cDNA cloning (Takeshima *et al.*, 1989; Zorzato *et al.*, 1990; Otsu *et al.*, 1990; Nakai *et al.*, 1990) of skeletal- and cardiac-muscle ryanodine receptor (RyR)–Ca^{2+}-release channels. These studies have shown that skeletal- and cardiac-muscle RyR channels are similar, but distinct, proteins that comprise homotetrameric 30 S complexes of $M_r \sim 565000$ subunits with pI ~ 4 (Lai *et al.*, 1989). The four subunits form into four-leaf-clover-like (quatrefoil) patterns that display a morphology identical with the 'feet' structures that bridge the T–SR junctional gap (Ferguson *et al.*, 1984). The isolated and reconstituted skeletal- and cardiac-muscle RyR channels can be activated Ca^{2+} ions, ATP and caffeine, and inhibited by Mg^{2+} ions and Ruthenium Red, as has been demonstrated for the native SR Ca^{2+}-release channel (Smith *et al.*, 1985, 1986; Rousseau *et al.*, 1986). Low concentrations of ryanodine modify the RyR channels into a permanently open state of decreased (about half) conductance, whereas higher concentrations of ryanodine cause the closing of the channel (Rousseau *et al.*, 1987; Lai *et al.*, 1989).

The second messenger, IP_3, has also been shown to cause the release of Ca^{2+} ions from intracellular membrane compartments of both excitable and non-excitable tissues (Berridge & Irvine, 1984, 1989). A homotetrameric IP_3 receptor (IP_3R) complex comprising subunits of $M_r \sim 320000$ has been isolated from mammalian cerebellum and smooth muscle (Supattapone *et al.*, 1988; Chadwick *et al.*, 1990; Maeda *et al.*, 1991). Reconstitution studies have shown the purified cerebellar IP_3R channel to behave differently from the muscle RyR channel with regard to unitary conductance and pharmacology (Ferris *et al.*, 1989). Single-channel measurements have indicated that the IP_3-sensitive Ca^{2+} channel has a fourfold lower conductance for Ca^{2+} ions than the RyR channel (~ 25 pS versus ~ 100 pS), and can be activated by IP_3 and inhibited by heparin (Erlich & Watras, 1988; Maeda *et al.*, 1991; Bezprozvanny *et al.*, 1991). Determination of the cerebellar IP_3R primary structure has revealed its homology with the muscle RyR (Furuichi *et al.*, 1989; Mignery *et al.*, 1990), suggesting that both are members of a new class of intracellular Ca^{2+} channels (Gill, 1989).

Although much effort has focused on the role of the RyR–Ca^{2+}-release channel in muscle E–C coupling, recent evidence has indicated that in mammalian brain, in addition to the IP_3R

Abbreviations used: E–C, excitation–contraction; SR, sarcoplasmic reticulum; RyR, ryanodine receptor; IP_3, inositol 1,4,5-trisphosphate; IP_3R, IP_3 receptor; PMSF, phenylmethanesulphonyl fluoride; STE, 0.5 M-NaCl/10 mM-Tris/HCl (pH 8)/1 mM-EDTA; SSC, 0.15 M-NaCl/15 mM-sodium citrate/HCl, pH 7; PBS, phosphate-buffered saline; WB – C, whole brain minus cerebellum; mAb, monoclonal antibody.

‡ To whom correspondence should be addressed, in London.

channel, there also exists a ryanodine-sensitive Ca^{2+} channel. Ryanodine binding, sedimentation and immunoblot analysis, as well as single-channel measurements with brain microsomes, have shown that a high-affinity brain RyR shares many of the characteristics of muscle Ca^{2+}-release channels (Ashley, 1989; Lai *et al.*, 1990; McPherson & Campbell, 1990; McPherson *et al.*, 1991). In this report, we describe studies of the brain RyR–Ca^{2+}-release channel complex that provide novel evidence for expression and localization of the cardiac RyR isoform in mammalian brain.

EXPERIMENTAL

Preparation of bovine brain and cerebellum microsomes

Bovine cerebellum and whole brain minus cerebellum (WB – C) were homogenized (Waring blender, 2 × 30 s, high) in 10 vol. of buffer A [0.32 M-sucrose, 10 mM-Pipes (sodium salt), pH 7.4, 0.5 mM-EDTA, 0.2 mM-phenylmethanesulphonyl fluoride (PMSF), 1 mM-benzamidine, 10 μM-leupeptin, 1 μM-pepstatin A and 100 nM-aprotinin]. Homogenates were centrifuged for 20 min at 4000 *g* (Sorvall GSA), and the supernatant passed through three layers of cheesecloth and re-centrifuged for 60 min at 100000 *g* (Beckman, Ti45 rotor). The 100000 *g* pellets were resuspended in 4 vol. of buffer A without EDTA, and loaded on to a 20–40 % linear sucrose gradient in 0.6 M-KCl/10 mM-Pipes (potassium salt), (pH 7)/0.2 mM-PMSF/1 μM-leupeptin, and centrifuged for 16 h at 130000 *g* (Beckman, SW28). Cerebellum and WB – C microsomes sedimenting to the 25–35 % sucrose region were diluted with 2 vol. of 0.4 M-KCl, pelleted at 100000 *g* and resuspended in 0.3 M-sucrose/5 mM-Pipes (potassium salt), (pH 7), and stored in approx. 5 ml portions at −75 °C. All procedures were performed at 4 °C.

[^{3}H]Ryanodine binding

Bovine cerebellum and WB – C microsomes (2–5 mg/ml) were incubated with various concentrations of [^{3}H]ryanodine as specified in the Figure legends, in buffer B [1.0 M-NaCl, 5 mM-AMP, 1 mM-di-isopropyl fluorophosphate, 10 μM-leupeptin, 20 mM-Pipes (sodium salt), pH 7.0] for 3 h at 37 °C. Samples of the vesicle suspensions were then (i) counted to determine total radioactivity, (ii) centrifuged for 30 min at 90000 *g* (Beckman Airfuge) to determine free [^{3}H]ryanodine and (iii) filtered, after dilution with 25 vol. of ice-cold water, on a Whatman GF/B filter disc soaked in 1 % polyethyleneimine. After three 5 ml rinses with ice-cold water, filters were counted to obtain a value for bound [^{3}H]-ryanodine. Non-specific binding of [^{3}H]ryanodine was assessed in the presence of a 1000-fold excess of unlabelled ryanodine and was equivalent to 0.3 pmol/mg of protein at 40 nM-[^{3}H]-ryanodine.

Purification of bovine brain RyR

Bovine WB – C microsomes (3 mg of protein/ml) were solubilized in buffer C (buffer B plus 100 μM-EGTA, 200 μM-Ca^{2+} and 0.3 mM-dithiothreitol) containing 120 nM-[^{3}H]ryanodine, 1.55 % Chaps and 5 mg of phosphatidylcholine/ml, for 2 h at 23 °C. Solubilized proteins (3 ml, 2.5 mg of protein/ml) were loaded on to a 9 ml cushion of 7 % sucrose in buffer C plus 1 % Chaps and 5 mg of phosphatidylcholine/ml, above a 24 ml 10–20 % linear sucrose gradient in buffer C plus 0.5 % Chaps and 5 mg of phosphatidylcholine/ml. Gradients were centrifuged for 16 h at 130000 *g*, 2 °C (Beckman SW28). Fractions of approx. 2 ml were collected, analysed for [^{3}H]ryanodine content, and the ~ 30 S [^{3}H]RyR peak fractions were pooled and concentrated (Centriprep 30, Amicon). Concentrates were diluted to approx. 5 % sucrose in buffer C plus 0.1 % Chaps, then loaded (2 ml) on to a second 10–20 % linear sucrose gradient (34 ml in buffer C plus 1 % Chaps). After centrifugation, fractionation and analysis of [^{3}H]ryanodine content, the fractions were concentrated separately. Skeletal- and cardiac-muscle RyRs were isolated as previously described (Lai *et al.*, 1988*a*,*b*; Anderson *et al.*, 1989).

Antibody production

Polyclonal antiserum (G715) against purified rat skeletal-muscle RyR was raised in rabbits, as previously described (Meissner *et al.*, 1989). Cardiac monoclonal antibodies (mAbs) were produced in Balb/c mice immunized with purified canine cardiac RyR (Anderson *et al.*, 1989). Immunized mouse spleen cells were fused with P3X 63AG 8.653 myeloma cells at a 1:1 ratio. Hybridoma supernatants were screened by e.l.i.s.a. using purified dog cardiac RyR, and by immunoblotting with dog cardiac microsomal SR as described below. Immunoblot analyses and immunolocalization studies with cardiac RyR-specific antibodies described in this report were performed with mAbs C2-997 and C3-33 of the IgM and IgG1 subtype respectively. Rabbit antiserum to mouse brain IP_3R *C*-terminus peptide was a gift from Dr. T. C. Südhof (Mignery *et al.*, 1989).

SDS/PAGE and immunoblot analysis

SDS/PAGE was performed (Laemmli, 1970) using 3–12 % (w/v) linear polyacrylamide gradient and 3 % (w/v) stacking gels. Samples were denatured for 3 min at 95 °C in 0.1 M-Tris/HCl (pH 6.8)/2 % SDS/3 % 2-mercaptoethanol/10 % glycerol. The acrylamide/bisacrylamide ratio was 39:1. Gels were either stained with Coomassie Brilliant Blue R-250 or silver (Oakley *et al.*, 1980).

Proteins for immunoblot analysis were transferred to Immobilon poly(vinylidene difluoride) membranes (Millipore) at 15 °C, for 1 h at 400 mA, then at 1500 mA for 12–15 h. Transfer membranes were blocked with 5 % non-fat dried-milk proteins, then probed with either skeletal RyR antiserum G715 (1:100 and 1:1000), cardiac RyR mAb (hybridoma supernatants, 1:10) or IP_3R antiserum (1:500), as previously described (Meissner *et al.*, 1989). Blots were developed with peroxidase-coupled secondary antibodies and 3,3′-diaminobenzidine/H_2O_2.

Electron microscopy

Bovine WB–C RyR purified as described above except in the absence of exogenous phospholipid was analysed by negative-stain electron microscopy. A sample (5 μl) of purified RyR was applied to a carbon-coated grid, previously glow-discharged, washed with three drops of 2 % uranyl acetate and air-dried. Quatrefoil images were recorded at 80 kV using a Zeiss 902 electron microscope at a magnification of × 85000.

Single-channel recordings

Single-channel measurement of bovine brain RyR channels was performed using the planar lipid-bilayer technique as described for purified muscle RyRs (Lai *et al.*, 1988*a*,*b*; Anderson *et al.*, 1989). Chaps-solubilized brain 30 S fractions from a single gradient, isolated in the absence of [^{3}H]ryanodine, were incorporated into Mueller–Rudin-type bilayers containing phosphatidylethanolamine, phosphatidylserine and phosphatidylcholine in the proportions 5:3:2 (by wt.; in *n*-decane). Samples of protein (0.2–2 μl) were added to one side (defined as *cis*) of the bilayer apparatus. Unless otherwise indicated, symmetrical solutions of buffered KCl [250 mM-KCl, 20 mM-Pipes (potassium salt), pH 7.0, 150 μM-$CaCl_2$ and 100 μM-EGTA] were used to record channel currents. Channels incorporating spontaneously into the bilayer were detected as stepwise increases in current. Electrical signals were filtered at 300 Hz and digitized at 2 kHz for storage on a hard disc.

Immunolocalization

Intact male rats (approx. 250 g) were perfused with 2% (v/v) paraformaldehyde in 10 mM-sodium phosphate buffer, pH 7.4, followed by 10% sucrose in phosphate-buffered saline (PBS; 0.15 M-NaCl and 10 mM-sodium phosphate), pH 7.4, under chloral hydrate anaesthesia. Brains were dissected, incubated in PBS containing 15% (w/v) sucrose, then frozen in liquid N_2-cooled isopentane. Serial frozen sections (8–10 μm) were thaw-mounted on to gelatin-coated slides and stored at −20 °C before avidin–biotin peroxidase immunostaining (Sar, 1985; Sar *et al.*, 1987). Sections were air-dried and incubated with 1–5 μg/ml of affinity-purified mouse IgG1 mAb C3-33 to the dog cardiac RyR, for 16–20 h at 4 °C. Slides were then washed in PBS and incubated with biotinylated anti-mouse IgG (1:200) and then with avidin–peroxidase (1:200) (Vector Labs) for 30 min at 23 °C. After being washed with PBS, sections were developed in 3,3′-diaminobenzidine/H_2O_2 for 10 min, dried and mounted with permount.

Hybridization *in situ*

A human cardiac RyR cDNA (nucleotides 3644–5500) cloned into Bluescript II (Stratagene, La Jolla, CA, U.S.A.) was linearized with *Bam*HI or *Eco*RV. Antisense and sense RNA probes were labelled with digoxigenin–UTP by transcription *in vitro* according to the Boehringer digoxigenin–RNA-labelled kit. Digoxigenin–RNA probes were cut to an average length of 180 bp by alkaline hydrolysis before use (Cox *et al.*, 1984).

Adult rat brains were bisected sagittally and immediately frozen in powdered dry ice. Sagittal sections (10 μm) collected on gelatin-chrome alum-coated slides, were dried and fixed in 4% paraformaldehyde/PBS, pH 7.4, for 1–2 h at 23 °C. Sections were dehydrated in an ascending series of alcohol and stored dry at −70 °C until use. Slides were rehydrated through a descending series of alcohol to PBS, treated with proteinase K (10 μg/ml) for 5 min, then refixed in 4% paraformaldehyde/PBS, pH 7.4, for 20 min, and acetic anhydride for 10 min at 23 °C (Wilkinson *et al.*, 1987). After dehydration as above, slides were hybridized overnight at 45 °C with digoxigenin-labelled cardiac-muscle RyR RNA probe (5 μg/ml) in 25 μl of hybridization mixture (Xue *et al.*, 1990). Sections were washed in 4 × SCC for 5, 15 and 30 min at 23 °C and treated with 20 μg of RNAase A/ml in 0.5 M-NaCl/10 mM-Tris/HCl (pH 8)/1 mM-EDTA (STE), for 30 min at 37 °C. After further washes in STE for 30 min at 37 °C, 2 × SSC for 30 min at 45 °C and twice in 0.1 × SSC for 15 min at 55 °C, each section was finally dehydrated as above and air-dried. Digoxigenin-labelled RNA was immunologically detected according to the Boehringer digoxigenin–RNA-labelling kit, but with 10% skimmed milk in 0.1 M-Tris/HCl (pH 7.5)/0.15 M-NaCl as the blocking agent.

Northern-blot analysis

Bovine brain (10 μg), cardiac (1 μg) and skeletal (1 μg) muscle poly(A)$^+$ RNA was fractionated on a 0.8% denaturing agarose/formaldehyde gel and transferred to Genescreen membrane (NEN–Dupont) under alkaline conditions (Sambrook *et al.*, 1989). Blots were hybridized with [α-^{32}P]dCTP-labelled cDNA probes (1 × 10^9 d.p.m./μg; Feinberg & Vogelstein, 1984) from the human cardiac RyR (nucleotides 3644–5500) or rabbit skeletal-muscle RyR (nucleotides 2547–4717), in 1% SDS/1 M-NaCl/10% dextran sulphate/10 μg of denatured salmon sperm/ml at 65 °C for 18 h. Washes for 30 min with 2 × SSC and then 0.1 × SSC at room temperature were performed before autoradiography on Fuji RX film.

Materials

[^{3}H]Ryanodine (54.7 Ci/mmol) was obtained from DuPont–New England Nuclear and ryanodine from Agrisystems International (Wind Gap, PA, U.S.A.). Peroxidase-conjugated secondary antibodies were from Calbiochem, Chaps and RNA-labelling kit from Boehringer-Mannheim, proteinase inhibitors and SDS/polyacrylamide gel standards from Sigma, and phospholipids from Avanti Polar Lipids (Birmingham, AL, U.S.A.).

RESULTS

[^{3}H]Ryanodine binding to bovine brain microsomes

Previous studies with skeletal- and cardiac-muscle SR indicated that high-affinity ryanodine binding is dependent on [Ca^{2+}] and ionic strength (Lai & Meissner, 1989). Scatchard analysis of ryanodine binding to WB−C microsomes, under optimal conditions for binding to muscle RyRs (100 μM free Ca^{2+} and 1 M-NaCl), indicated the presence of a single high-affinity site with a K_d of 3 nM and $B_{max.}$ of 0.25 pmol/mg (Fig. 1*a*). Fewer specific binding sites were observed with bovine cerebellum microsomes, where [^{3}H]ryanodine-binding studies resulted in a $B_{max.}$ value of

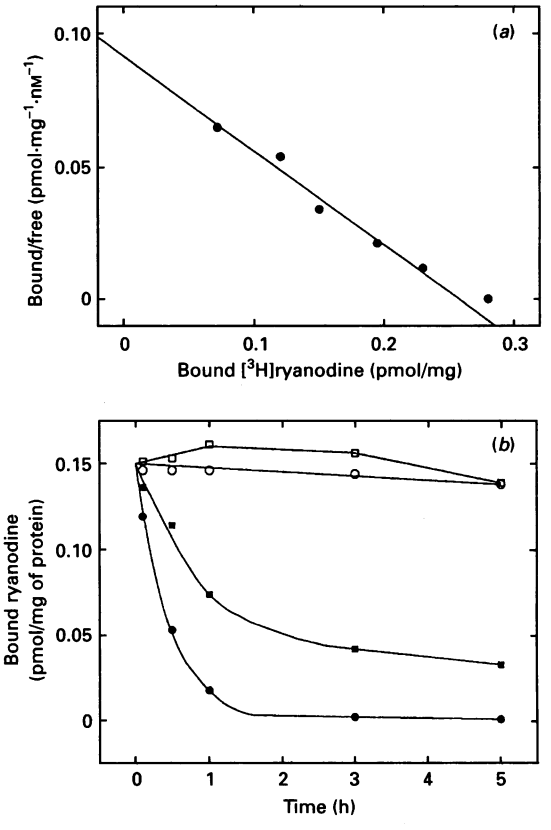

Fig. 1. Ryanodine binding to bovine whole-brain microsomes

(*a*) Scatchard analysis of [^{3}H]ryanodine binding. Bovine WB−C microsomes (2 mg of protein/ml) were incubated for 3 h at 37 °C in buffer B containing 100 μM-EGTA, 200 μM-Ca^{2+} and 1–40 nM-[^{3}H]ryanodine. Specific [^{3}H]ryanodine binding was determined as described in the Experimental section. (*b*) Rate of [^{3}H]ryanodine dissociation with or without 200 μM-ryanodine. Bovine WB−C microsomes (5 mg of protein/ml) were incubated for 3 h at 37 °C in buffer B containing 100 μM-free Ca^{2+} and 18 nM-[^{3}H]ryanodine. Dissociation of [^{3}H]ryanodine from the high-affinity site was initiated by diluting microsomes 10-fold into medium B at 37 °C containing the indicated concentrations of free Ca^{2+} and unlabelled ryanodine. Bound ryanodine was determined at various times as described in the Experimental section. ●, 0.01 μM-Ca^{2+}; ○, 0.01 μM-Ca^{2+} + 200 μM-ryanodine; ■, 100 μM-Ca^{2+}; □, 100 μM-Ca^{2+} + 200 μM-ryanodine.

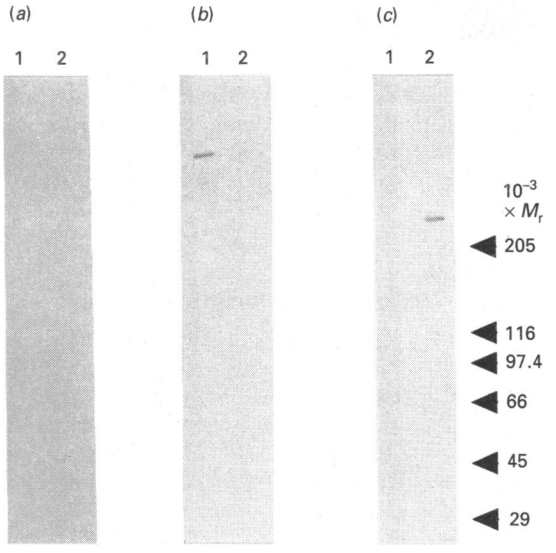

Fig. 2. Immunoblot analysis of bovine whole brain and cerebellum microsomes

Bovine WB−C (lane 1) and cerebellum (lane 2) microsomes were electrophoresed through SDS/polyacrylamide gels (3–12% gels) (100 μg of protein/lane in *a* and *b*, 20 μg/lane in *c*), transferred to Immobilon membrane, and probed with skeletal-muscle RyR antiserum G715 (*a*), cardiac-muscle RyR mAb C2-997 (*b*) or IP_3R antiserum (*c*). Solid arrowheads indicate the positions of M_r standards ($\times 10^{-3}$) myosin, β-galactosidase, phosphorylase *b*, BSA, ovalbumin and carbonic anhydrase in order of decreasing M_r.

< 0.02 pmol/mg (results not shown). In studies with muscle SR, ryanodine sites of low affinity have been identified in addition to the high-affinity site (Lai *et al.*, 1989; McGrew *et al.*, 1989; Pessah & Zimanyi, 1991). Occupation of low-affinity sites decreased the dissociation rate of bound ryanodine from high-affinity site, suggesting that co-operative interactions occurred between high- and low-affinity sites. To determine whether a similar phenomenon existed with the brain RyR, we tested for low-affinity sites by initially labelling WB−C microsomes with [^{3}H]ryanodine in 100 μM free Ca^{2+} to optimize high-affinity binding. Labelled membranes were diluted into 0.01 μM free Ca^{2+} with or without 200 μM unlabelled ryanodine or 100 μM free Ca^{2+} with or without 200 μM unlabelled ryanodine (Fig. 1*b*). Dilution into 0.01 μM free Ca^{2+}, a concentration that minimizes rebinding of dissociated [^{3}H]ryanodine, resulted in loss of bound [^{3}H]ryanodine within 1 h. Dilution into 100 μM free Ca^{2+}, a condition that favours high-affinity binding, resulted in incomplete dissociation of bound [^{3}H]ryanodine, due to partial rebinding of dissociated [^{3}H]ryanodine. In contrast, a dramatic decrease in [^{3}H]ryanodine dissociation from the high-affinity site was observed under both conditions when 200 μM unlabelled ryanodine was present in the dilution medium. These studies suggest that brain RyRs, like muscle RyRs, possess both high- and low-affinity ryanodine-binding sites. Further, the [^{3}H]ryanodine-displacement data suggest positive co-operativity between these classes of binding site (Lai *et al.*, 1989), in which occupation of low-affinity sites results in conformational change(s) that occludes dissociation from the high-affinity site.

Immunoblot analysis of brain and cerebellum microsomes

Fig. 2 shows the distribution of RyRs and IP_3Rs in bovine cerebellum and WB−C microsomes, as detected by immunoblot analysis with antiserum to skeletal-muscle RyR (Fig. 2*a*), mAb to cardiac-muscle RyR (Fig. 2*b*) and antiserum to cerebellum IP_3R (Fig. 2*c*). No immunoreactivity to WB−C or cerebellum proteins was observed with a mammalian skeletal-muscle RyR

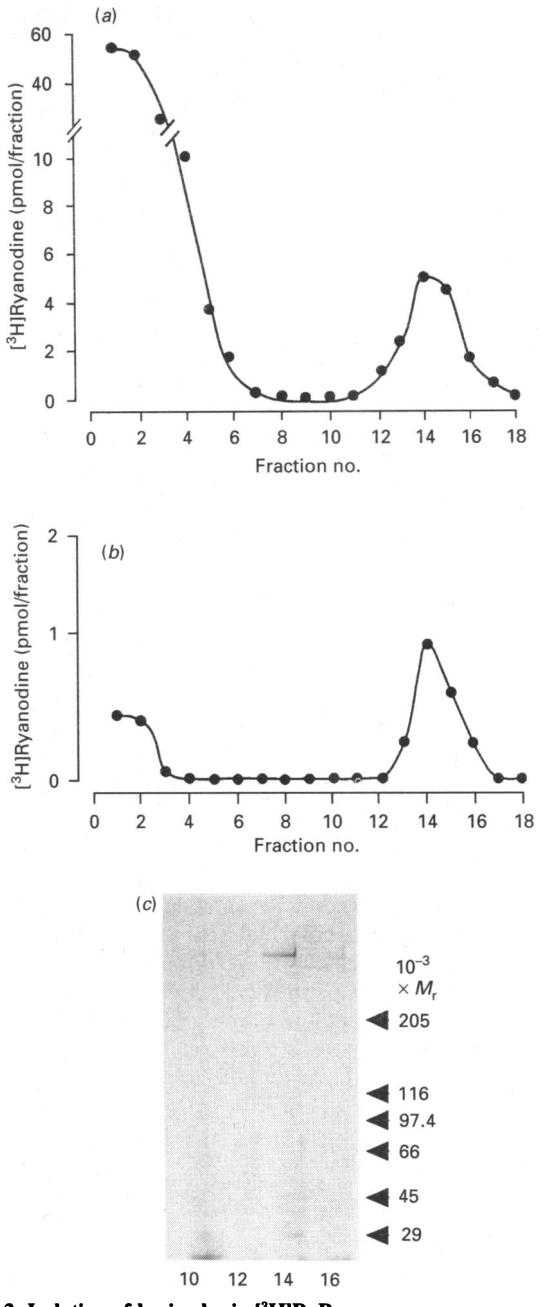

Fig. 3. Isolation of bovine brain [^{3}H]RyR

(*a*, *b*) Gradient sedimentation profiles of bovine brain RyR. Chaps-solubilized WB−C microsomes were centrifuged on linear 10–20% sucrose gradients and the approx. 30 S [^{3}H]RyR peak fractions 13–16 pooled and concentrated. Concentrated fractions from (*a*) were re-centrifuged on a second 10–20% linear sucrose gradient, and the ~ 30 S fractions (10–16) concentrated separately. (*c*) SDS/polyacrylamide gel of [^{3}H]ryanodine peak fractions from gradient (*b*). Samples of concentrated fractions (100 μl) were electrophoresed through SDS/3–12% polyacrylamide gradient gels and stained with Coomassie Brilliant Blue. Solid arrowheads indicate positions of M_r standards as in Fig. 2.

antiserum (Fig. 2*a*). Blots probed with a mAb to mammalian cardiac-muscle RyR, however, revealed a single immunoreactive high-M_r band in WB−C, but not cerebellum, microsomes (Fig. 2*b*). Conversely, an immunoreactive band corresponding to the cerebellum IP_3R (Supattapone *et al.*, 1988) was observed when cerebellum microsomes were probed with IP_3R antiserum (Fig. 2*c*). The immunoblot data suggest a relative enrichment of cardiac mAb-immunoreactive RyR in WB−C microsomes, in

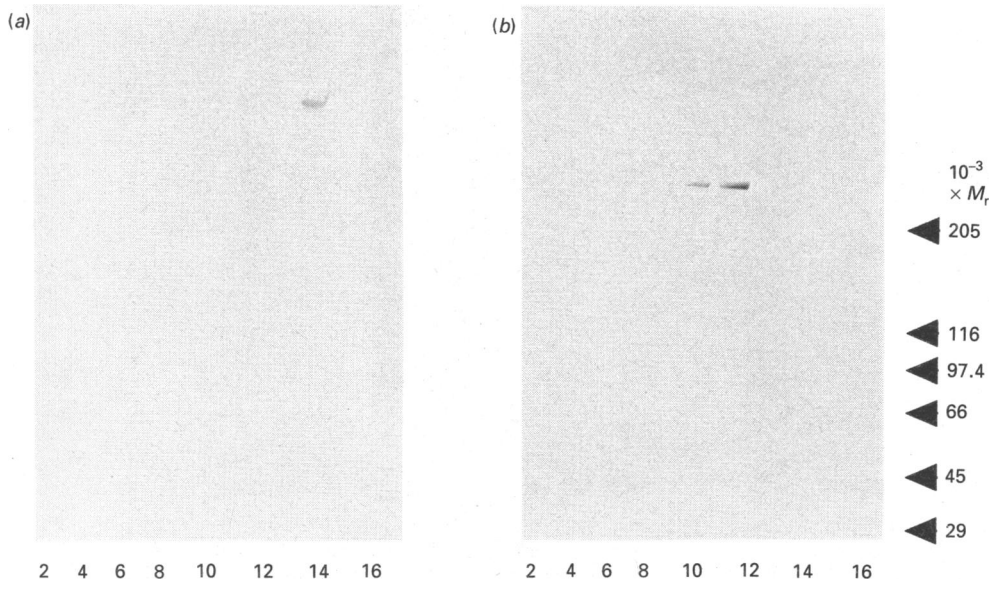

Fig. 4. Immunoblot analysis of sucrose-gradient fractions

Samples (120 μl) of sucrose-gradient fractions, obtained with bovine WB−C (*a*) and cerebellum (*b*) microsomes as described in Fig. 3, were electrophoresed through 3–12% gradient gels, and transferred to Immobilon membranes. The WB−C blot was probed with cardiac-muscle RyR mAb C2-997 (*a*), and the cerebellum blot with IP_3R antiserum (*b*). Solid arrowheads indicate positions of M_r standards as in Fig. 2.

agreement with ryanodine-binding data described above. In contrast, the IP_3R is enriched in cerebellar microsomes, in agreement with previous reports of IP_3-binding studies (Worley *et al.*, 1987; Supattapone *et al.*, 1988).

Purification of bovine brain RyR and immunoblot analysis

The [^{3}H]ryanodine-labelled brain RyR was isolated from bovine WB−C microsomes by centrifugation through sucrose-density gradients as described for skeletal- and cardiac-muscle RyRs (Lai *et al.*, 1988*a*,*b*; Anderson *et al.*, 1989). The [^{3}H]-ryanodine peak of Chaps-solubilized WB−C microsomes, migrating with apparent sedimentation coefficient ~ 30 S, was isolated by a double-sucrose-gradient procedure (Figs. 3*a* and 3*b*). SDS/PAGE analysis of the second gradient revealed specific co-migration of a single high-M_r band with the [^{3}H]ryanodine peak (Fig. 3*c*). Immunoblot analysis showed that the single high-M_r band immunoreactive with cardiac-muscle mAb was present only in the ~ 30 S [^{3}H]ryanodine peak (Fig. 4*a*). The sedimentation profile of this high-M_r band migrating at ~ 30 S was clearly different from that of the cerebellar IP_3R, which migrated in identical gradients at ~ 24 S (Fig. 4*b*). The mobility of the large polypeptide co-migrating with the [^{3}H]ryanodine peak (R_F = 0.12, Fig. 3*c*) was identical with the immunoreactive band observed in WB−C microsomes (Fig. 2*b*) and ~ 30 S peak fractions (Fig. 4*a*). Protein determination yielded 16 μg of purified brain RyR from 45 mg of WB−C protein. Assuming a single high-affinity site per ~ 30 S complex and M_r equivalent to the muscle RyR (2.3×10^6), the ryanodine-binding density of WB−C microsomes (Fig. 1*a*) indicates a quantitative receptor yield of 25 μg (0.05% of WB−C protein). The observed yield of 16 μg represents an overall protein recovery of 64%. [^{3}H]-Ryanodine binding to the purified unlabelled receptor was not quantified because of the low amounts of protein recovered.

Comparison of purified brain, cardiac- and skeletal-muscle RyRs

SDS/PAGE analysis of purified brain RyR on 3–12% gels (Fig. 5) revealed a single high-M_r band (lane 3) that displayed an identical mobility with the purified cardiac-muscle RyR (lane 4). Both brain and cardiac-muscle RyR bands (R_F = 0.12) migrated with a relative mobility greater than that of the purified skeletal-muscle RyR (R_F = 0.10, lane 5). Earlier studies have shown the

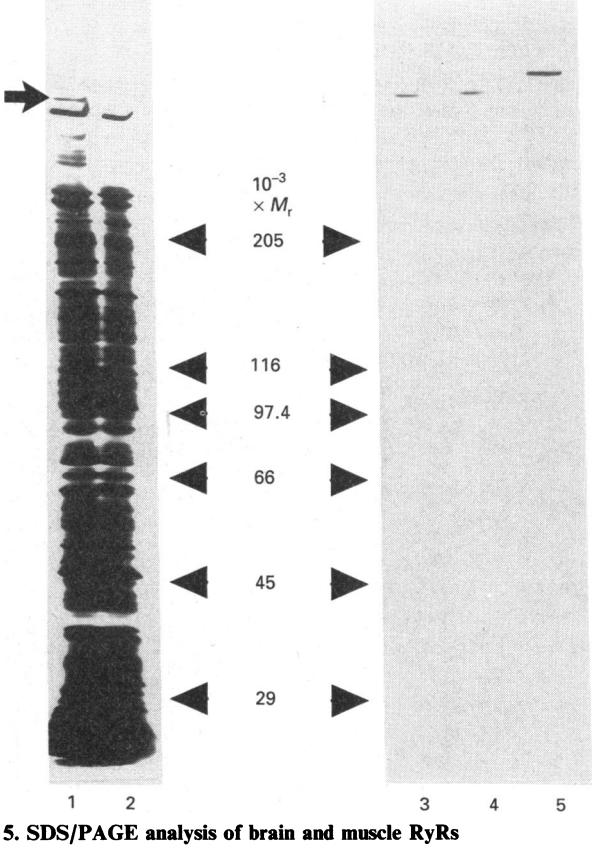

Fig. 5. SDS/PAGE analysis of brain and muscle RyRs

Microsomes from bovine WB−C (lane 1; 15 μg of protein) and cerebellum (lane 2; 15 μg), and the purified 30 S RyR from bovine WB−C microsomes (lane 3; 0.5 μg), dog-cardiac-muscle SR (lane 4; 0.5 μg), and rabbit skeletal-muscle SR (lane 5; 2 μg) were electrophoresed through 3–12% gradient gels and stained with silver. Solid arrowheads indicate positions of M_r standards as in Fig. 2.

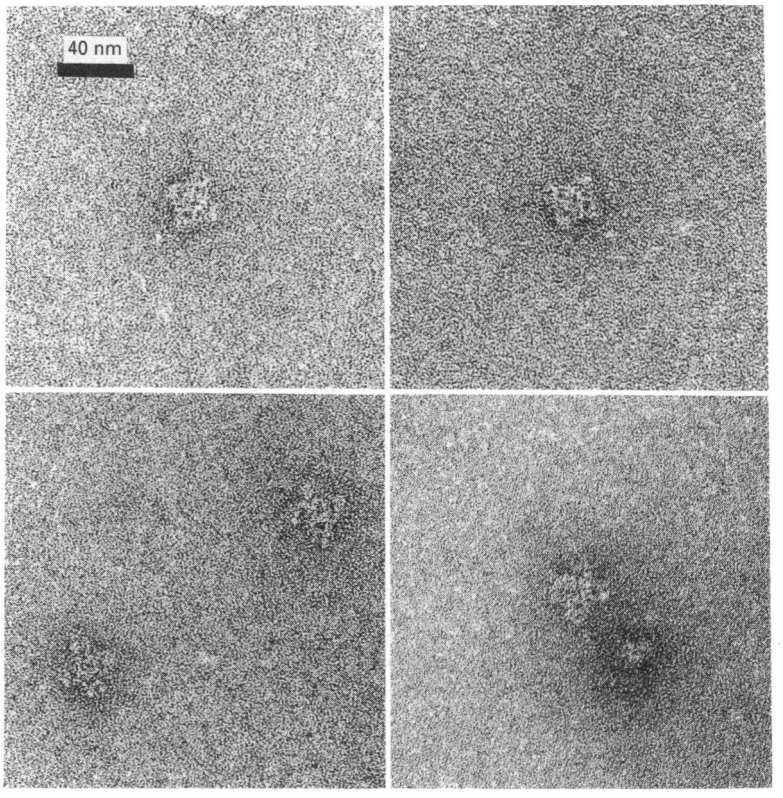

Fig. 6. Morphology of the purified bovine brain RyR

Bovine WB – C RyR isolated in the absence of exogenous phospholipid was analysed by negative-stain electron microscopy. A montage of selected quatrefoil images of the brain RyR is shown. Scale bar represents 40 nm.

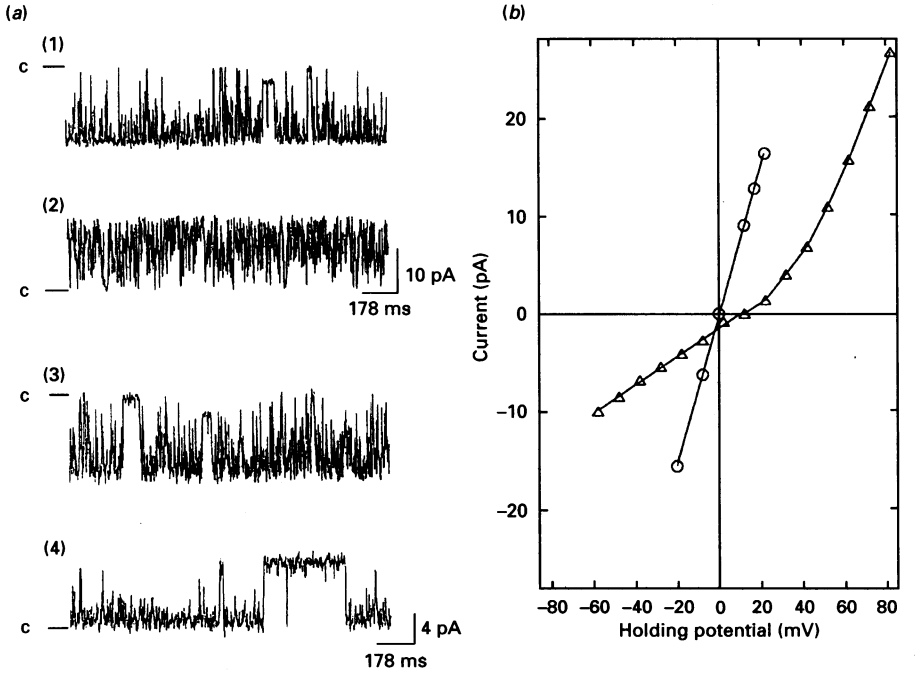

Fig. 7. Single-channel currents of bovine brain RyR complex reconstituted into a planar lipid bilayer

Bovine WB – C RyR isolated as described in Fig. 3(*a*) was incorporated into planar lipid bilayers for single-channel analysis. Upward deflections represent channel openings. The baseline current is denoted by the bar to the left of the trace, labelled c (for channel closed state). (*a*) Traces 1 and 2, single-channel K^+ currents recorded in symmetrical 0.25 M-KCl buffer containing 50 μM free Ca^{2+}. Holding potentials are +20 mV and −20 mV respectively. Traces 3 and 4, single-channel Ca^{2+} and K^+ currents recorded after perfusion of the *trans* chamber with 50 mM-$CaCl_2$. Holding potentials are +52 mV and −48 mV respectively. (*b*) Current–voltage relationship. ○, K^+ current: unitary conductance is 800 ± 32 pS (±S.D., $n = 15$). (△), currents obtained after perfusing *trans* chamber with 50 mM-$CaCl_2$, unitary Ca^{2+} conductance is 140 pS.

cardiac-muscle RyR R_F is slightly higher than that of skeletal-muscle RyR (Inui *et al.*, 1987*b*; Lai *et al.*, 1988*a*), although subsequent cDNA sequence analysis predicts similar M_r values of approx. 565000 for the two rabbit muscle RyR isoforms (Takeshima *et al.*, 1989; Zorzato *et al.*, 1990; Otsu *et al.*, 1990; Nakai *et al.*, 1990).

Analysis of WB–C (lane 1) and cerebellar (lane 2) microsomes revealed a minor band of high M_r in WB–C membranes (arrow; $R_F = 0.12$), which corresponded in mobility to the purified brain RyR (lane 3). The low abundance of this protein correlates with the 0.05% relative RyR content derived from ryanodine-binding studies described above. Further, this minor band was not apparent in the cerebellum lane loaded at an identical protein concentration (lane 2), in concert with our ryanodine-binding data indicating a more than 10-fold lower RyR concentration in cerebellum than in WB–C microsomes.

Electron microscopy of brain RyR

Brain RyR isolated in the absence of exogenous phospholipid was examined by negative-stain electron microscopy. Fig. 6 illustrates selected enlarged images of bovine brain RyR displaying the presence of four-leaf clover-like (quatrefoil) structures characteristic of skeletal- and cardiac-muscle RyRs (Lai *et al.*, 1988*b*; Anderson *et al.*, 1989; Wagenknecht *et al.*, 1989), and morphologically identical with the 'feet' structures spanning the T–SR junctional gap (Ferguson *et al.*, 1984). The brain RyR quatrefoil from the tip of one leaf to the tip of the opposite one is ~ 34 nm, with each leaf ~ 13 nm in diameter. Stain accumulations of ~ 3 nm diameter were apparent at the centre of each leaf. In addition, a central depression or hole of 1–2 nm was apparent at the centre of the complex surrounded by a ring, ~ 12 nm diameter, of higher protein density. This central ~ 12 nm region of the quatrefoil has been suggested to form the transmembrane channel-forming domain of the muscle RyR (Lai *et al.*, 1988*b*; Wagenknecht *et al.*, 1989).

Single-channel recordings of brain RyR

Brain RyRs were reconstituted into planar lipid bilayers in symmetric 0.25 M-KCl buffer containing 50 μM free Ca^{2+}. Use of symmetric univalent cation buffers has been shown to facilitate reconstitution of skeletal- and cardiac-muscle RyR channels (Lai *et al.*, 1988*b*; Liu *et al.*, 1989*a*; Anderson *et al.*, 1989). Also, univalent cations give currents of larger amplitude than those observed when using Ca^{2+} ions as the current carrier. Fig. 7*a* (upper two recordings) shows current traces from an incorporated single channel after addition of the channel protein to the cis chamber. The channel was partially activated at positive and negative holding potentials, and displayed a unitary K^+ conductance of 800 pS (Fig. 7*b*). The two lower recordings of Fig. 7(*a*) show the current traces obtained after perfusion of the trans chamber with 50 mM-Ca^{2+}. The current–voltage plot under these conditions (Fig. 7*b*) indicates a unitary Ca^{2+} conductance of 140 pS. By using identical recording conditions, unitary conductances for skeletal- and cardiac-muscle Ca^{2+}-release channels of 770 and 745 pS for K^+ ions, and 145 and 148 pS for Ca^{2+} ions respectively were obtained. From the reversal potential of +10 mV observed after trans chamber perfusion with Ca^{2+}, a permeability ratio for Ca^{2+} versus K^+ ions (P_{Ca}/P_K) of 6.5 was calculated for the reconstituted brain RyR channel.

Pharmacology of brain RyR channel

The pharmacological responses of the brain RyR channel after the successive addition of various agents are illustrated in recordings from a single reconstituted channel (Fig. 8). Trace 1 shows a K^+-conducting channel in 50 μM free Ca^{2+}. As observed for skeletal- and cardiac-muscle RyR channels, the open probability (P_o) of the brain channel decreased on lowering *cis* free Ca^{2+} from 50 μM to 90 nM (trace 2), and could subsequently be elevated to half the control value by raising *cis* free Ca^{2+} to 1.7 μM (trace 3). In traces 4–6, the sensitivity of the Ca^{2+}-activated channel to IP_3 and heparin was tested. On addition of 0.3 μM-IP_3 *cis*, a 2-fold increase in P_o was observed (trace 4). Further increase in IP_3 *cis* to 10 μM resulted in a decrease in channel activity (trace 5). Heparin addition to 1 mg/ml *cis* was without a significant effect (result not shown). However, further addition of heparin to 2 mg/ml *cis* greatly decreased channel activity (trace 6). Partial activation of the channel by millimolar concentrations of ATP was evident in trace 7. The extent of channel activation by ATP illustrated in trace 7, however, was less than that obtained in other recordings, where P_o values usually increased from ~ 0.3 (in 50 μM free Ca^{2+}) to ~ 0.9 on addition of millimolar ATP *cis* (not shown). Traces 8 and 9 confirm the identity of the reconstituted brain protein as a ryanodine-sensitive channel. On addition of 10 μM-ryanodine *cis*,

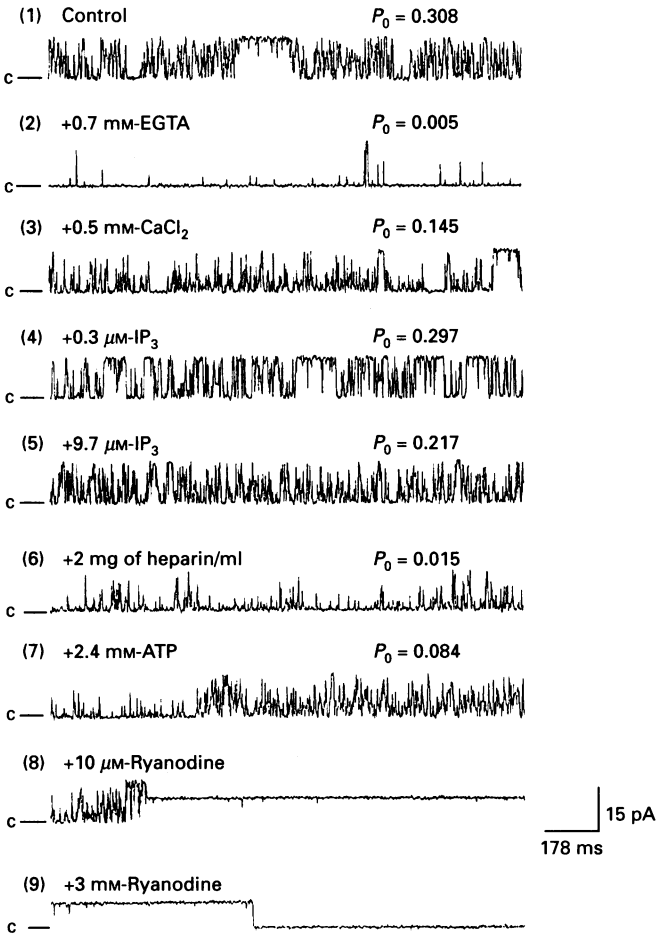

Fig. 8. Pharmacological responses of bovine brain RyR channel

Single-channel currents, shown as upward deflections, were recorded in symmetrical 0.25 M-KCl buffer. The baseline current is denoted by the bar to the left of the trace, denoted c (for closed channel state). Holding potential = −20 mV. Trace 1, 50 μM free Ca^{2+} *cis*, $P_o = 0.308$. Trace 2, 91 nM free Ca^{2+} *cis*, $P_o = 0.005$. Trace 3, 1.7 μM free Ca^{2+} *cis*, $P_o = 0.145$. Trace 4, after addition of 0.3 μM-IP_3 *cis*, $P_o = 0.297$. Trace 5, after addition of IP_3 to 10 μM *cis*, $P_o = 0.217$. Trace 6, after addition of 2 mg of heparin/ml *cis*, $P_o = 0.015$. Trace 7, after addition of 2.4 mM-ATP *cis*, $P_o = 0.084$. Trace 8, after addition of 10 μM-ryanodine *cis*, channel entered modified conductance state. Trace 9, after addition of ryanodine to 3 mM *cis*, channel entered closed state. Similar effects to these were observed in three different experiments.

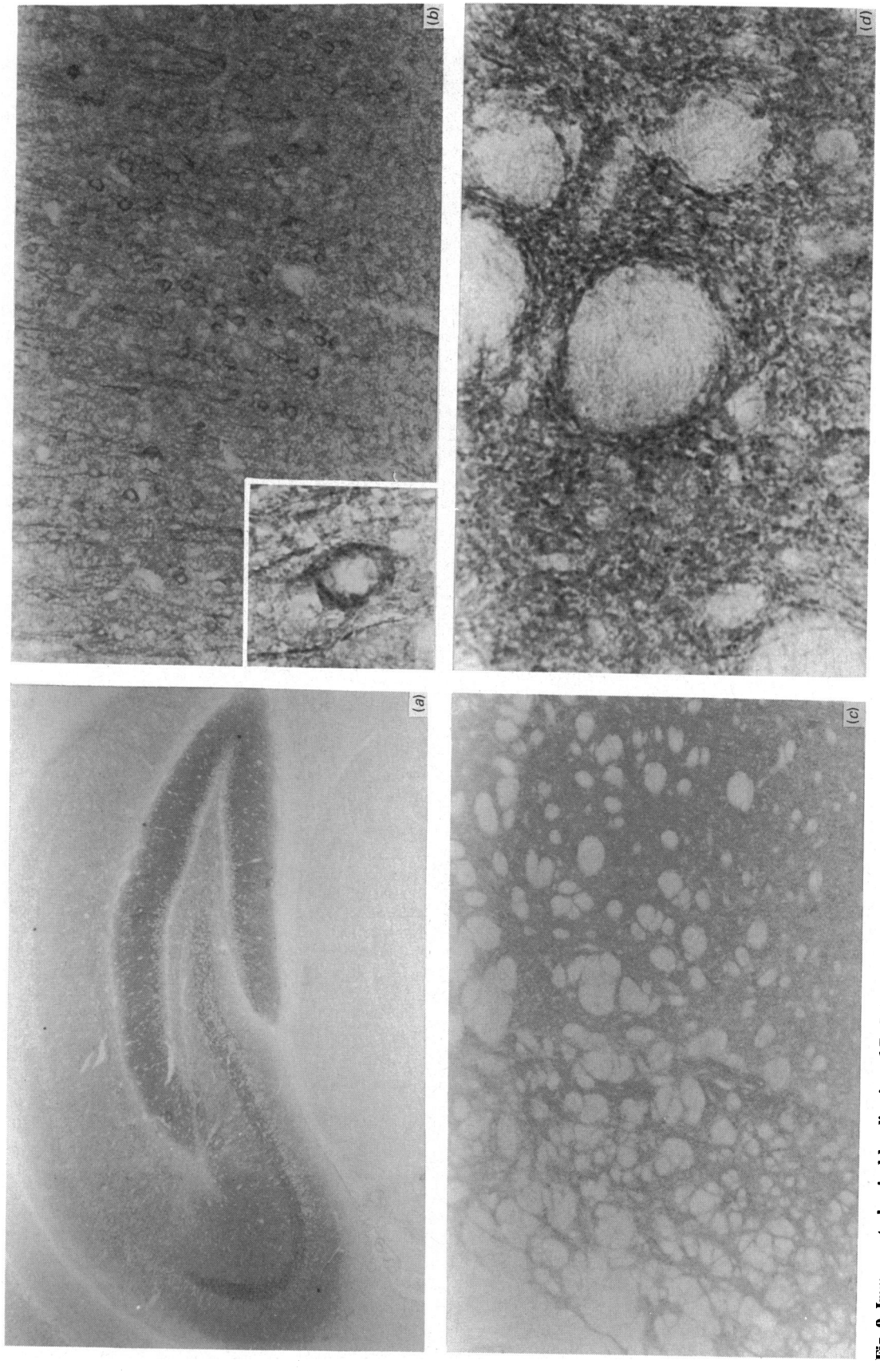

Fig. 9. Immunocytochemical localization of RyR in rat brain

Serial frozen sections of rat brain were immunostained with affinity-purified IgG1 mAb C3-33 specific for the cardiac-muscle RyR. Immunostaining patterns observed in the hippocampus (*a*; ×30), cortex (*b*; ×60) and caudate-putamen (*c*; ×60 and *d*; ×590) are shown. Inset in *b* is a higher magnification (×590) of a single perikaryon.

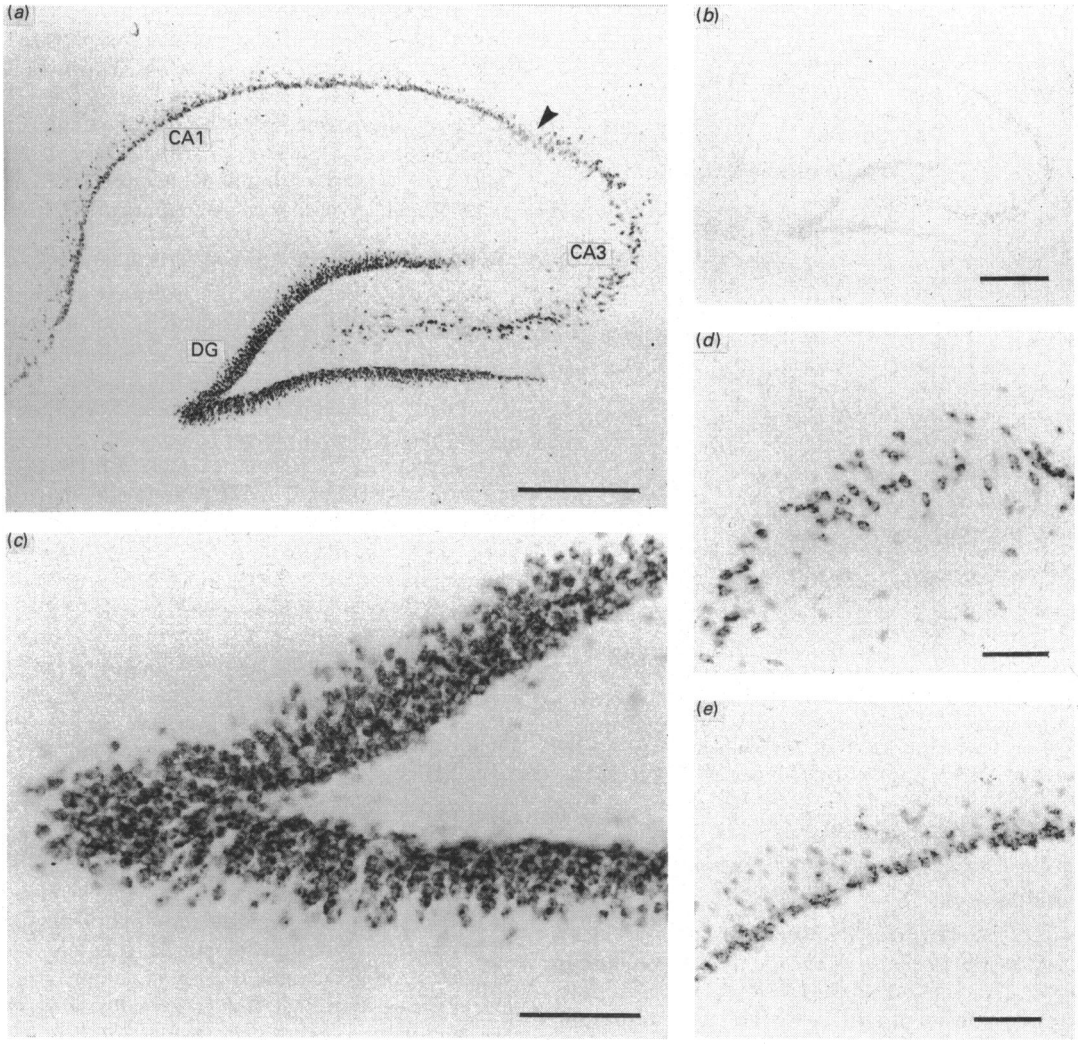

Fig. 10. Localization *in situ* of RyR mRNA in rat hippocampus

Sagittal sections of rat brain were hybridized with digoxigenin-labelled cardiac-muscle RyR RNA. Hybridization pattern of the hippocampus with antisense RNA probe (*a*) and sense RNA probe (*b*) are shown. Enlarged views of dentate gyrus (DG) granule cells (*c*), and pyramidal cells of hippocampal fields CA3 (*d*), and CA1 (*e*) are taken from (*a*). The arrowhead in (*a*) shows the junction between CA1 and CA3. Scale bars in (*a*) and (*b*) = 500 μm, and those in (*c*), (*d*) and (*e*) = 100 μm.

the characteristic formation of a fully open channel state of decreased conductance was observed (trace 8). The order of IP_3 and ryanodine addition was not changed, because ryanodine modification renders the channel insensitive to regulation by most effector molecules (Rousseau *et al.*, 1987). In the presence of 3 mM-ryanodine *cis*, the channel abruptly closed and remained inactive for the remainder of the recording (trace 9). Identical effects of low and high concentrations of ryanodine have been shown for the bilayer reconstituted muscle RyR channel (Lai *et al.*, 1989).

Localization of brain RyR

Immunocytochemical localization of the mammalian brain RyR using a cardiac-muscle RyR mAb revealed its wide distribution throughout adult rat forebrain (Fig. 9). Immunoreactive regions of the brain were hippocampus (Fig. 9*a*), cortex (Fig. 9*b*), caudate-putamen (Figs. 9*c* and 9*d*), septum, amygdala, olfactory bulb, thalamus and hypothalamus. High levels of RyR immunoreactivity were found throughout the cortex and dentate gyrus of the hippocampus. Immunostain was observed in the layers of dendrites and cell bodies (Fig. 2*b* and inset), and in the region corresponding to mossy fibres (Fig. 9*a*). By comparison, and in accord with our [^{3}H]ryanodine-binding studies, there appeared to be less immunoreactivity in the mammalian cerebellum, including the Purkinje cells (not shown). No staining of brain sections was observed in controls using either mouse IgG or after preabsorption of mAb with purified cardiac-muscle RyR (not shown).

Hybridization *in situ* of cardiac-muscle RyR antisense RNA to sagittal sections of adult rat brain indicated that RyR RNA expression was widely distributed throughout the brain, and was particularly enriched in the hippocampal formation. Fig. 10 illustrates the abundant expression of RyR RNA in the hippocampus. Localization of RyR RNA to the pyramidal layers of hippocampal fields CA1 and CA3 (Figs. 10*a*, 10*d* and 10*e*), with even higher levels present in the granule cell layer of the dentate gyrus (Figs. 10*a* and 10*c*), was apparent. Hybridization with the control RNA sense strand revealed little signal, even in layers of hippocampus that are densely packed with neuronal cell bodies (Fig. 10*b*). In agreement with our [^{3}H]ryanodine-binding and immunolocalization studies, there appeared to be lower levels of RyR RNA in the mammalian cerebellum (result not shown).

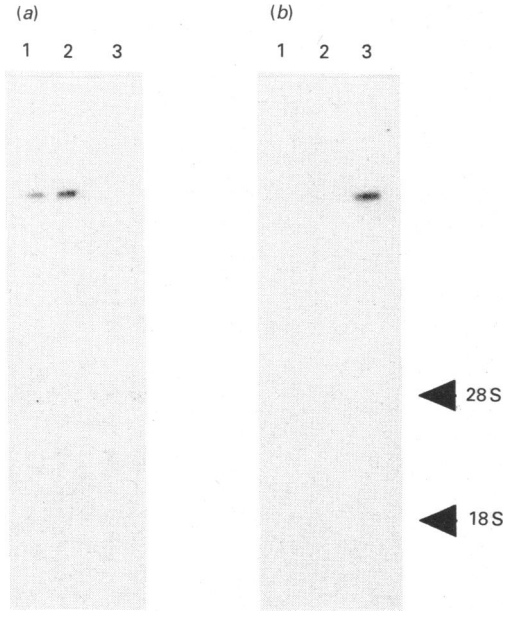

Fig. 11. Northern-blot analysis

Poly(A)$^+$ RNA from bovine brain (lane 1), cardiac muscle (lane 2) and skeletal muscle (lane 3) was electrophoresed through a 0.8% agarose gel and transferred to Genescreen membrane. Blots were hybridized with mammalian cDNA probes derived from the cardiac-muscle RyR (*a*) or skeletal-muscle RyR (*b*), as described in the Experimental section. Solid arrowheads indicate positions of yeast 18 S and 28 S RNA standards.

Northern-blot analysis

mRNA isolated from bovine whole brain, skeletal- and cardiac-muscle tissue was hybridized to cDNA probes specific for the mammalian cardiac- or skeletal-muscle RyR (Fig. 11). Both bovine cardiac-muscle and brain mRNA contained a transcript of approx. 16 kb which hybridized specifically with a cardiac-muscle cDNA probe (Fig. 11*a*). A cardiac RyR mRNA of approx. 16 kb has previously been identified in rabbit heart (Otsu *et al.*, 1990; Nakai *et al.*, 1990). In contrast, hybridization of the skeletal-muscle RyR cDNA probe to an approx. 16 kb band was observed only with skeletal-muscle mRNA (Fig. 11*b*). An approx. 16 kb skeletal-muscle RyR mRNA has been shown in rabbit and human skeletal muscle (Takeshima *et al.*, 1989; Zorzato *et al.*, 1990). These hybridization data (Fig. 11) suggest that a cardiac RyR-specific mRNA is expressed in brain.

DISCUSSION

Evidence for a brain RyR

Early morphological observations on rat brain by Henkart *et al.* (1976) identified the presence of bridging structures between surface and intracellular membranes, with an arrangement and dimensions similar to the 'feet' structures found between the T- and SR membranes in muscle. Evidence for a ryanodine- and caffeine-sensitive intracellular Ca^{2+} store was subsequently demonstrated in rat sympathetic neurons using fluorimetric and electrophysiological measurements of intracellular Ca^{2+} (Thayer *et al.*, 1988*a*,*b*; Lipscombe *et al.*, 1988), suggesting the existence of an intracellular Ca^{2+} channel in brain with properties similar to the muscle SR Ca^{2+} channel. Ashley (1989) described binding of [^{3}H]ryanodine to a high-affinity site of K_d approx. 3 nM in rat brain microsomes. Incorporation of the rat brain microsomes into planar lipid bilayers resulted in the appearance of a Ca^{2+}-conducting channel that could be activated by ATP, caffeine and IP_3. Ryanodine transformed the rat brain channel into a state of lower conductance (Ashley, 1989), as previously observed for Ca^{2+}-release channels of muscle SR (Rousseau *et al.*, 1987; Lai *et al.*, 1989). RNA-blot analysis using a cardiac-muscle RyR cDNA probe detected a low-abundance mRNA of approx. 16 kb in rabbit brain (Otsu *et al.*, 1990). These previous studies are all in accord, suggesting that an RyR is present in mammalian brain with properties similar to the mammalian muscle RyRs.

Brain RyR–Ca^{2+}-release channel is a cardiac isoform

Earlier biochemical studies indicated the presence of a mammalian brain RyR with an apparent sedimentation coefficient of approx. 30 S comprising high-M_r subunits (Lai *et al.*, 1990; McPherson & Campbell, 1990; McPherson *et al.* 1990), identical with that observed for skeletal- and cardiac-muscle RyRs (Lai *et al.*, 1988*b*; Anderson *et al.*, 1989). Immunoblot analysis showed cross-reactivity of selected skeletal-muscle RyR antisera and a peptide antiserum to a high-M_r band from rabbit brain that migrated close to the skeletal-muscle RyR (McPherson & Campbell, 1990; McPherson *et al.*, 1991). However, the lack of immunoreactivity to the brain RyR of other skeletal-muscle RyR antisera (Fig. 2*a*; McPherson & Campbell, 1990), and of skeletal-muscle RyR-specific mAbs (McPherson and Campbell, 1990; F. A. Lai, unpublished work), indicates that the brain RyR, although similar to, is not identical with the skeletal-muscle RyR. In the present study, we have identified the 30 S bovine brain RyR channel complex to display an immunological cross-reactivity specifically to cardiac-muscle RyR mAbs (Figs. 2*b* and 4*a*), and an electrophoretic mobility identical with that of the purified cardiac RyR (Figs. 3*c* and 5). Northern-blot hybridization analysis with a cardiac RyR-specific cDNA probe reveals specific labelling of a 16 kb transcript in bovine brain mRNA (Fig. 11). Brain mRNA did not hybridize to skeletal-muscle RyR-specific cDNA probes under identical conditions. These studies strongly suggest that mammalian brain specifically expresses a cardiac RyR–Ca^{2+}-release channel isoform, although we cannot at present exclude the possibility of a distinct neuronal RyR isoform. Table 1 summarizes the properties of the 30 S RyR isolated from bovine brain, dog cardiac muscle and rabbit skeletal muscle. All three RyRs exist as tetrameric complexes of high-M_r subunits arranged into a four-leaf-clover pattern. The RyR channels readily conduct univalent cations with a large unitary conductance of 700–800 pS for K^+ ions, and possess low- and high-affinity ryanodine-binding sites, occupation of which results in disparate effects on single-channel conductance. RyR channel activity can be increased by micromolar concentrations of Ca^{2+} and millimolar concentrations of ATP, and decreased by millimolar concentrations of Mg^{2+} and micromolar concentrations of Ruthenium Red.

IP_3 effect on brain RyR channel

Single-channel recordings of the microsomal (Ashley, 1989), and solubilized (Fig. 8), brain RyR incorporated into a planar lipid bilayer indicate that cis addition of low concentrations of IP_3 can weakly activate channel opening. Only at high concentrations of heparin, in excess of 1 mg/ml, could the IP_3 activation be reversed (Fig. 8). In contrast, IP_3 binding and activation of the cerebellar IP_3R could be fully inhibited by heparin concentrations of 100 μg/ml (Ferris *et al.*, 1989). The basis for this common observation of activation of RyR and IP_3R channels by IP_3 is unclear at present. Although significant sequence similarity is present within the putative transmembrane channel-forming domain at the *C*-terminus of the RyR and IP_3R (Furuichi *et al.*, 1989), the structure(s) within the IP_3R involved in IP_3 binding is now believed to include the *N*-terminus (Mignery & Südhof, 1990; Miyawaki *et al.*, 1991), where sequence similarity

Table 1. Comparison of properties of ryanodine receptors purified from bovine brain, dog cardiac muscle and rabbit skeletal muscle

N.D., not determined.

Property	Brain	Cardiac muscle	Skeletal muscle
1. Apparent sedimentation coefficient	30 S	30 S†	30 S‡
2. R_F in SDS/3–12% polyacrylamide gels	0.12	0.12	0.10
3. Morphology	Quatrefoil	Quatrefoil†	Quatrefoil‡
4. Calculated subunit M_r ($\times 10^{-3}$) (from cDNA sequence)	N.D.	565§	564‖
5. Ryanodine binding.			
High-affinity (K_d)	3 nM	3 nM†	6 nM¶
Low-affinity	Yes	Yes**	Yes¶
6. Ryanodine modification	Yes	Yes†	Yes¶
Sublevel conductance state (μM)			
Closing of channel (mM)	Yes	N.D.	Yes¶
7. Single-channel conductance*			
In 0.25 M-K^+	800 pS	745 pS	770 pS
In 0.05 M-Ca^{2+}	140 pS	148 pS	145 pS
8. Regulation			
Activation by Ca^{2+} and ATP	Yes	Yes†	Yes‡
Activation by IP_3	Occasional	N.D.	Occasional††
Inhibition by Mg^{2+} and Ruthenium Red	Yes	Yes†	Yes‡

* Measured using conditions described in Fig. 7(*b*).
† Data from Anderson *et al.* (1989).
‡ Data from Lai *et al.* (1988*b*).
§ Data from Otsu *et al.* (1990) and Nakai *et al.* (1990).
‖ Data from Takeshima *et al.* (1989) and Zorzato *et al.* (1990).
¶ Data from Lai *et al.* (1989).
** Data from Pessah & Zimanyi (1991).
†† Data from Liu *et al.* (1989*b*).

with the RyR is lower. A similar weak activation of RyR channels purified from mammalian and amphibian muscle, by cis addition of IP_3, has also been observed (Suarez-Isla *et al.*, 1988; Liu *et al.*, 1989*b*). Conversely, ATP, a potent muscle RyR channel activator (Meissner, 1984; Smith *et al.*, 1985), has been shown to stimulate the purified cerebellum IP_3R channel (Ferris *et al.*, 1989; Maeda *et al.*, 1991), and calmodulin, a muscle RyR channel antagonist (Meissner, 1986), also interacts with the purified IP_3R (Maeda *et al.*, 1991). These similarities in the pharmacological profile of the RyR and IP_3R channels are consistent with those observed for their sedimentation behaviour (Fig. 4), morphology (Fig. 6; Chadwick *et al.*, 1990), subunit structure (Lai *et al.*, 1989; Maeda *et al.*, 1991) and primary structure (Furuichi *et al.*, 1989; Mignery *et al.*, 1989). However, no effect of ryanodine on the IP_3R channel incorporated into planar lipid bilayers has yet been reported. One distinctive difference observed in single-channel recordings of the IP_3R and RyR was the lower permeability to univalent cations of the reconstituted IP_3R channel. The unitary conductance for Na^+ ions of 21 pS in 100–500 mM-Na^+ for the IP_3R channel (Maeda *et al.*, 1991) is in contrast with the value of 400 pS observed for the skeletal RyR under similar recording conditions (Smith *et al.*, 1988; Liu *et al.*, 1989*a*).

Localization of brain RyR

Localization of the mammalian brain RyR by immunocytochemistry and hybridization *in situ* using cardiac-muscle RyR-specific mAb and antisense RNA respectively revealed prominent reactivity in the hippocampal formation, particularly in the molecular layer of the dentate gyrus and in the terminals of cells projecting from this area into the CA3 field of the hippocampus (Figs. 9 and 10). This hippocampal enrichment in RyR is in accord with observations from ryanodine-binding studies to membrane fractions isolated from various rabbit brain regions (McPherson & Campbell, 1990), and with [^{3}H]ryanodine autoradiography (Padua *et al.*, 1991), indicating brain RyR was particularly enriched in the hippocampus. The studies by hybridization *in situ* (Fig. 11) complement the immunocytochemical analysis (Fig. 10) and indicate markedly high levels of RyR RNA expression in the granule cells of dentate gyrus with a lower level of expression in the pyramidal cells of the CA3 and CA1 field of the hippocampus. The functional significance of these observations is not known, although the importance of intracellular Ca^{2+} stores was demonstrated in a recent study which showed that in cultured *Xenopus* spinal neurons, Ca^{2+}-induced release of Ca^{2+} promotes cell differentiation (Holliday *et al.*, 1991). This Ca^{2+}-sensitive mechanism of intracellular Ca^{2+} release is in concurrence with our observation that the brain RyR channel is a cardiac-specific isoform.

A recent immunocytochemical study of the avian cerebellum RyR has shown it to be enriched in the Purkinje neurons (Ellisman *et al.*, 1990), as has been found for the IP_3R (Ross *et al.*, 1989). The avian cerebellum Purkinje neuron RyR was localized by immunogold electron microscopy to the smooth and rough endoplasmic reticulum and subsurface membrane cisternae, and found to co-localize with IP_3Rs throughout the Purkinje neuron, with the exception of dendritic spines where only the IP_3Rs were evident (Walton *et al.*, 1991). In contrast, our ryanodine-binding and localization data indicate that expression of the mammalian RyR and IP_3R in cerebellum and whole brain displays an inverse relationship, with the RyR in mammalian cerebellum present at approx. 10-fold lower concentrations than in the rest of the brain. The relatively disperse distribution of the neuronal RyR within intracellular membrane compartments of the Purkinje neuron (Walton *et al.*, 1991), in comparison with specific localization of muscle RyR to the T–SR junctions (Ferguson *et al.*, 1984), makes the assignment of a plausible role for this intracellular channel more challenging.

Studies of the skeletal- and cardiac-muscle RyR channels have indicated that they are coupled to a sarcolemmal voltage-sensing and a Ca^{2+}-induced Ca^{2+}-release mechanism respectively (Rios & Pizarro, 1988). Our observations that the brain RyR channel is a cardiac isoform, and likewise sensitive to activation by micromolar concentrations of Ca^{2+}, would suggest a role of Ca^{2+} ions in regulating this channel, possibly via the Ca^{2+}-induced Ca^{2+}-release mechanism (Thayer *et al.*, 1988*a*,*b*; Lipscombe *et al.*, 1988; Holliday *et al.*, 1991) that predominates during E–C coupling in cardiac cells (Cannell *et al.*, 1987; Näbauer *et al.*, 1989). In conclusion, the studies reported here suggest that the RyR present in brain probably plays an important role in neuronal intracellular Ca^{2+} homoeostasis generally, and may be of particular significance in the regulation of Ca^{2+} levels pre- and post-synaptically.

We are grateful for the generous gift of IP_3R peptide antiserum from Dr. Thomas C. Südhof, University of Texas Southwestern Medical Center, Dallas, TX, U.S.A., and to Dr. John Seeley, National Institute for Medical Research, London, U.K. for helpful discussions. This work was supported by U.S.P.H.S. grants AR18687, HL27430 and GM30598 and by the British Heart Foundation.

REFERENCES

Anderson, K., Lai, F. A., Liu, Q. Y., Rousseau, E., Erickson, H. P. & Meissner, G. (1989) J. Biol. Chem. **264**, 1329–1335

Ashley, R. H. (1989) J. Membr. Biol. **111**, 179–189
Berridge, M. J. & Irvine, R. F. (1984) Nature (London) **312**, 315–321
Berridge, M. J. & Irvine, R. F. (1989) Nature (London) **341**, 197–205
Bezprozvanny, I., Watras, J. & Ehrlich, B. E. (1991) Nature (London) **351**, 751–754
Campbell, K. P., Knudson, C. M., Imagawa, T., Leung, A. T., Sutko, J. L., Kahl, S. D., Raab, C. R. & Madson, L. (1987) J. Biol. Chem. **262**, 6460–6463
Cannell, M. B., Berlin, J. & Lederer, W. J. (1987) Science **238**, 1419–1423
Catterall, W. A. (1991) Cell **64**, 871–874
Chadwick, C. C., Saito, A. & Fleischer, S. (1990) Proc. Natl. Acad. Sci. U.S.A. **87**, 2132–2136
Cox, H. K., DeLeon, D. V., Angerer, L. M. & Angerer, R. C. (1984) Dev. Biol. **101**, 485–502
Ehrlich, B. E. & Watras, J. (1988) Nature (London) **336**, 583–586
Ellisman, M. H., Deerinck, T. J., Ouyang, Y., Beck, C. F., Tanksley, S. J., Walton, P. D., Airey, J. A. & Sutko, J. L. (1990) Neuron **5**, 135–146
Feinberg, A. P. & Vogelstein, B. (1984) Anal. Biochem. **137**, 266–267
Ferguson, D. G., Schwartz, H. W. & Franzini-Armstrong, C. (1984) J. Cell Biol. **99**, 1735–1742
Ferris, C. D., Huganir, R. L., Supattapone, S. & Snyder, S. H. (1989) Nature (London) **342**, 87–89
Furuichi, T., Yoshikawa, S., Miyawaki, A., Wada, K., Maeda, N. & Mikoshiba, K. (1989) Nature (London) **342**, 32–38
Gill, D. L. (1989) Nature (London) **342**, 16–18
Henkart, M., Landis, D. M. D. & Reese, T. S. (1976) J. Cell Biol. **70**, 338–347
Holliday, J., Adams, R. J., Sejnowski, T. J. & Spitzer, N. C. (1991) Neuron **7**, 787–796
Inui, M., Saito, A. & Fleischer, S. (1987*a*) J. Biol. Chem. **262**, 1740–1747
Inui, M., Saito, A. & Fleischer, S. (1987*b*) J. Biol. Chem. **262**, 15637–15642
Laemmli, U. K. (1970) Nature (London) **227**, 680–685
Lai, F. A. & Meissner, G. (1989) J. Bioenerg. Biomemb. **21**, 227–246
Lai, F. A., Anderson, K. A., Rousseau, E., Liu, Q. Y. & Meissner, G. (1988*a*) Biochem. Biophys. Res. Commun. **151**, 441–449
Lai, F. A., Erickson, H., Rousseau, E., Liu, Q. Y. & Meissner, G. (1988*b*) Nature (London) **331**, 315–319
Lai, F. A., Misra, M., Xu, L., Smith, H. A. & Meissner, G. (1989) J. Biol. Chem. **264**, 16776–16785
Lai, F. A., Xu, L. & Meissner, G. (1990) Biophys. J. **57**, 529*a*
Lipscombe, D., Madison, D. V., Poenie, M., Reuter, H., Tsien, R. W. & Tsien, R. Y. (1988) Neuron **1**, 355–365
Liu, Q. Y., Lai, F. A., Rousseau, E., Jones, R. V. & Meissner, G. (1989*a*) Biophys. J. **55**, 415–424
Liu, Q. Y., Lai, F. A., Xu, L., Jones, R. V., LaDine, J. K. & Meissner, G. (1989*b*) Biophys. J. **55**, 85a
Maeda, N., Kawasaki, T., Nakade, S., Yokota, N., Taguchi, T., Kasai, M. & Mikoshiba, K. (1991) J. Biol. Chem. **266**, 1109–1116
Meissner, G. (1984) J. Biol. Chem. **259**, 2365–2374
Meissner, G. (1986) Biochemistry **25**, 244–251
Meissner, G., Rousseau, E. & Lai, F. A. (1989) J. Biol. Chem. **264**, 1715–1722
McGrew, S. G., Wolleben, C., Siegl, P., Inui, M. & Fleischer, S. (1989) Biochemistry **28**, 1686–1691
McPherson, P. S. & Campbell, K. P. (1990) J. Biol. Chem. **265**, 18454–18460
McPherson, P. S., Kim, Y. K., Valdivia, H., Knudson, C. M., Takekura, H., Franzini-Armstrong, C., Coronado, R. & Campbell, K. P. (1991) Neuron **7**, 17–25
Mignery, G. A. & Südhof, T. C. (1990) EMBO J. **9**, 3893–3898
Mignery, G. A., Südhof, T. C., Takei, K. & DeCamilli, P. (1989) Nature (London) **342**, 192–195
Mignery, G. A., Newton, C. L., Archer III, B. T. & Südhof, T. C. (1990) J. Biol. Chem. **265**, 12679–12685
Miyawaki, A., Furuichi, T., Ryou, Y., Yoshikawa, S., Nakagawa, T., Saitoh, T. & Mikoshiba, K. (1991) Proc. Natl. Acad. Sci. U.S.A. **88**, 4911–4915
Näbauer, M., Callewaert, G., Cleemann, L. & Morad, M. (1989) Science **244**, 800–803
Nakai, J., Imagawa, T., Hakamata, Y., Shigekawa, M., Takeshima, H. & Numa, S. (1990) FEBS Lett. **271**, 167–177
Oakley, B. R., Kirsch, D. R. & Morris, N. R. (1980) Anal. Biochem. **105**, 361–363
Otsu, K., Willard, H. F., Khanna, V. J., Zorzato, F., Green, N. M. & MacLennan, D. H. (1990) J. Biol. Chem. **265**, 13472–13483
Padua, R. A., Wan, W., Nagy, J. I. & Geiger, J. D. (1991) Brain Res. **542**, 135–140
Pessah, I. N. & Zimanyi, I. (1991) Mol. Pharmacol. **39**, 679–689
Rios, E. & Pizarro, G. (1988) News Physiol. Sci. **3**, 223–227
Ross, C. A., Meldolesi, J., Milner, T. A., Satoh, T., Supattapone, S. & Snyder, S. H. (1989) Nature (London) **339**, 468–470
Rousseau, E., Smith, J. S., Henderson, J. S. & Meissner, G. (1986) Biophys. J. **50**, 1009–1014
Rousseau, E., Smith, J. S. & Meissner, G. (1987) Am. J. Physiol. **253**, C364–C368
Sambrook, J., Fritsch, E. F. & Maniatis, T. (1989) Molecular Cloning. A Laboratory Manual, 2nd edn., Cold Spring Harbor Laboratory Press, Cold Spring Harbor, NY
Sar, M. (1985) in Techniques in Immunocytochemistry (Bulbele, G. R. & Petruez, P., eds), vol. 3, pp. 43–54, Academic Press, New York
Sar, M., Culler, M. D., McGimsey, W. C. & Negro-Vilar, A. (1987) Neuroendocrinology **45**, 180–192
Smith, J. S., Coronado, R. & Meissner, G. (1985) Nature (London) **316**, 446–449
Smith, J. S., Coronado, R. & Meissner, G. (1986) J. Gen. Physiol. **88**, 573–588
Smith, J. S., Imagawa, T., Ma, J., Fill, M., Campbell, K. P. & Coronado, R. (1988) J. Gen. Physiol. **92**, 1–26
Suarez-Isla, B. A., Irribara, V., Oberhauser, A., Larralde, L., Bull, R., Hidalgo, C. & Jaimovich, E. (1988) Biophys. J. **54**, 737–741
Supattapone, S., Worley, P. F., Baraban, J. M. & Snyder, S. H. (1988) J. Biol. Chem. **263**, 1530–1534
Takeshima, M., Nishimura, S., Matsumoto, T., Ishida, M., Kangawa, K., Minamino, N., Matsuo, H., Ueda, M., Hanaoka, M., Hirose, T. & Numa, S. (1989) Nature (London) **339**, 439–445
Thayer, S. A., Hirning, L. D. & Miller, R. J. (1988*a*) Mol. Pharmacol. **34**, 664–673
Thayer, S. A., Perney, T. M. & Miller, R. J. (1988*b*) J. Neurosci. **8**, 4089–4097
Wagenknecht, T., Grassuci, R., Frank, J., Saito, A., Inui, M. & Fleischer, S. (1989) Nature (London) **338**, 167–170
Walton, P. D., Airey, J. A., Sutko, J. L., Beck, C. F., Mignery, G. A., Südhof, T. C., Deerinck, T. J. & Ellisman, M. H. (1991) J. Cell Biol. **113**, 1145–1157
Wilkinson, D. G., Bailes, J. A., Champion, J. E. & McMahon, A. P. (1987) Development **99**, 493–500
Worley, P. F., Baraban, J. M., Supattapone, S., Wilson, V. S. & Snyder, S. H. (1987) J. Biol. Chem. **262**, 12132–12136
Xue, G. P., Calvert, R. A. & Morris, R. J. (1990) Development **109**, 851–864
Zorzato, F., Fujii, J., Otsu, K., Phillips, M., Green, N. M., Lai, F. A., Meissner, G. & MacLennan, D. H. (1990) J. Biol. Chem. **265**, 2244–2256

Received 13 April 1992/12 June 1992; accepted 22 June 1992